

行政院國家科學委員會專題研究計畫 成果報告

奈米結構異質接面高分子太陽能電池之材料開發及元件設計(3/3)

研究成果報告(完整版)

計畫類別：整合型
計畫編號：NSC 99-2120-M-009-003-
執行期間：99年08月01日至100年10月31日
執行單位：國立交通大學材料科學與工程學系(所)

計畫主持人：韋光華
共同主持人：黃中焄、林建村、鄭有舜

報告附件：國外研究心得報告
出席國際會議研究心得報告及發表論文

公開資訊：本計畫可公開查詢

中華民國 101 年 02 月 01 日

中文摘要：在這項研究中，我們用一層聚(3,4-乙烯基)：(苯乙烯磺酸鈉) (PEDOT:PSS) 電洞傳輸層，提升硒化鉛量子點 (QD) 太陽能電池元件在 AM1.5 標準頻譜下之光電轉換效率，從標準的硒化鉛量子點元件，效率由 1.5% 提升至 2.4%。利用同步輻射 X 射線反射測量顯示，各層之間的界面的粗糙度因存在的 PEDOT:PSS 層而急劇下降。此外，根據連續模擬 AM1.5 照射 (100mW/cm²) 元件的壽命時間，我們發現硒化鉛量子點結合的 PEDOT:PSS 薄膜元件在降低效率到原先的 80% 所需的時間是 6 倍以上的標準硒化鉛量子點元件。(Advanced Functional Materials, 2010, 20, 3555-3560)

我們已經使用了 Stille 聚合準備噻吩並 [3,4-C] 吡咯-4,6-二酮 (TPD) 基聚合物 PBTPD，具有優良的熱穩定性，結晶的特點，和較低的 HOMO 能階；這些理想的特性意味著 PBTPD 有潛力的聚合物太陽能電池的應用。通過元件結構與成分組成的優化製程，PBTPD / PCBM 太陽能電池元件 0.95V 的開路電壓，而整體的光電轉換效率為 4.7%。(Macromolecules, 2010, 43, 6936 - 6938)

我們在量子點太陽能電池元件的基礎上對 CdSe 四角錐狀和利用供體/受體的混摻膜結合共軛聚合物 PDTTPD，其中包括 2,5-二(2-噻吩基)噻吩並 [3,2-b]噻吩噻吩並 [3,4-C]吡咯-4,6-二酮單位。在 AM1.5 標準量測環境下的光電轉換效率 (PCE) 在與 CdSe 四角錐狀/ PDTTPD 的混合比為 1:9, W / W 的元件是 PDTTPD / 硒化鎘四角錐狀具有 1:1, W / W 混合 (2.9% 與 1.0%) 的三倍。同步輻射 X 射線反射顯示，退火造成 PDTTPD / 硒化鎘四角錐狀共混膜的減少相對的元件膜厚度。穿透式電子顯微鏡和原子力顯微鏡發現，熱退火的 CdSe 四角錐狀和形態的聚集程度會因退火而增強，導致大幅增加元件效率。(Energy Environ. Sci., 2011, 4, 2316 - 2322)

我們使用同步 GIWAXS/GISAXS 在即時同步調件下之分辨技術，我們已獲知 PCBM 聚集和相應的塊狀異質界面高分子太陽能電池的 P3HT 結晶動力學。PCBM 聚集的大小在 P3HT/PCBM 複合薄膜於熱退火 150°C 的條件下，從 7 奈米提升至 18 奈米，然後飽和迅速增長在 100 秒時間內，同時，多數 P3HT 與片狀大小，從 7 奈米增大至 12 奈米的大小。PCBM 聚集和 P3HT 結晶的動力學可利用特徵相似的 Avrami 指數近似逼近分析；我們發現更快 PCBM 聚集，有一個高 2 倍 Avrami 速率常數。相互密閉的增長導致可使 PCBM 和 P3HT 具有 20 奈米以下的奈米晶的大小，當退火溫度低於 180°C 下保持 PCBM 和 P3HT 奈米區塊的發展可能會強烈影響塊狀異質界面高分子太陽能電池的電子和電洞遷移率。元件構造在熱火

的製程中 P3HT/PCBM 膜的流動性的變化說明了動力學可能承擔相關的替代聚合物/富勒烯衍生物的組合選擇，並可在未來高分子太陽能電池的製程條件做出相關的貢獻。(ACS Nano, 2011, 5, 6233 - 6243)

中文關鍵詞：共軛導電高分子、高分子太陽能電池、硒化鎘、硒化鉛量子點、熱退火、結晶動力學

英文摘要：In this study, we used a thin poly(3,4-ethylenedioxythiophene):poly(styrene sulfonate) (PEDOT:PSS) hole transport layer enhances the AM1.5 power conversion efficiency of a PbSe quantum dot (QD) - containing photovoltaic device to 2.4%, from 1.5% for a standard PbSe QD device, a relative increase of 60%.
We have used Stille polymerization to prepare the thieno[3,4-c]pyrrole-4,6-dione (TPD)-based polymer PBTTTPD, which features excellent thermal stability, crystalline characteristics, and a low-lying HOMO energy level; these desirable properties mean that PBTTTPD has promising potential for application in polymer solar cells. Through devices' composition optimization, a device incorporating the PBTTTPD/PCBM blend at a weight ratio of 1:1.5 displayed an open-circuit voltage of 0.95 V and, therefore, a PCE of 4.7%.
We have prepared photovoltaic devices based on blend films of CdSe tetrapods and the donor/acceptor conjugated polymer PDTTTPD, which comprises 2,5-di(thiophen-2-yl)thieno[3,2-b]thiophene and thieno[3,4-c]pyrrole-4,6-dione units. The AM1.5 power conversion efficiency (PCE) of a photovoltaic device containing a PDTTTPD/CdSe tetrapod blend (1 : 9, w/w) was three times greater than that of the corresponding device incorporating the as-prepared PDTTTPD/CdSe tetrapod blend (2.9% vs. 1.0%).
We used synchronized GIWAXS and GISAXS of enhanced spatial/time resolutions, we have captured the competing kinetics of PCBM aggregation and P3HT crystallization of the corresponding BHJ thin-film solar cells. The developments of PCBM and P3HT nanodomains could influence strongly and sensitively the electron and hole mobilities of the BHJ thin-film

solar cells. The illustrated kinetics of structural evolution and its correlation to changes in charge mobility of P3HT/PCBM composite films may bear relevance to the selection of alternative polymer/fullerene derivative combinations and in the optimization of processing conditions for future BHJ thin-film solar cells.

英文關鍵詞： conducting conjugated polymer, polymer solar cell, CdSe, PbSe QDs, thermal annealing, crystalline kinetics

行政院國家科學委員會補助專題研究計畫 成果報告
 期中進度報告

奈米結構異質接面高分子太陽能電池之材料開發及元件設計

(3/3)

計畫類別： 個別型計畫 整合型計畫

計畫編號：NSC 99-2120-M-009-003 (99R445)

執行期間：97年8月1日至100年7月31日

執行機構及系所：國立交通大學材料科學與工程學系(所)

計畫主持人：交通大學材料系 韋光華教授
共同主持人：中央研究院化學所 林建村教授
交通大學光電所 黃中堦教授
國家同步輻射研究中心 鄭有舜博士
交通大學材料系 吳文偉助理教授

計畫參與人員：

成果報告類型(依經費核定清單規定繳交)： 精簡報告 完整報告

本計畫除繳交成果報告外，另須繳交以下出國心得報告：

- 赴國外出差或研習心得報告
 赴大陸地區出差或研習心得報告
 出席國際學術會議心得報告
 國際合作研究計畫國外研究報告

處理方式：除列管計畫及下列情形者外，得立即公開查詢

涉及專利或其他智慧財產權， 一年 二年後可公開查詢

中 華 民 國 年 月 日

Abstract

In this study, we used a thin poly(3,4-ethylenedioxythiophene):poly(styrene sulfonate) (PEDOT:PSS) hole transport layer enhances the AM1.5 power conversion efficiency of a PbSe quantum dot (QD)-containing photovoltaic device to 2.4%, from 1.5% for a standard PbSe QD device, a relative increase of 60%. Synchrotron X-ray reflectivity measurements reveal that the roughness of the interfaces between the various layers decreases dramatically in the presence of the PEDOT:PSS layer. In addition, the device life time under continuous simulated AM1.5 irradiation (100 mW cm^{-2}), measured in terms of the time required to reach 80% of the normalized efficiency, for the PbSe QD device incorporating the PEDOT:PSS hole transport layer is six times longer than that of the standard PbSe QD device.

We have used Stille polymerization to prepare the thieno[3,4-*c*]pyrrole-4,6-dione (TPD)-based polymer PBTTTPD, which features excellent thermal stability, crystalline characteristics, and a low-lying HOMO energy level; these desirable properties mean that PBTTTPD has promising potential for application in polymer solar cells. Through devices' composition optimization, a device incorporating the PBTTTPD/PCBM blend at a weight ratio of 1:1.5 displayed an open-circuit voltage of 0.95 V and, therefore, a PCE of 4.7%.

We have prepared photovoltaic devices based on blend films of CdSe tetrapods and the donor/acceptor conjugated polymer PDTTTPD, which comprises 2,5-di(thiophen-2-yl)thieno[3,2-*b*]thiophene and thieno[3,4-*c*]pyrrole-4,6-dione units. The AM1.5 power conversion efficiency (PCE) of a photovoltaic device containing a PDTTTPD/CdSe tetrapod blend (1 : 9, w/w) was three times greater than that of the corresponding device incorporating the as-prepared PDTTTPD/CdSe tetrapod blend (2.9% vs. 1.0%). Synchrotron X-ray reflectivity revealed that annealing caused the thickness of the PDTTTPD/CdSe tetrapod blend film to decrease relative to that of the as-prepared blend film. Transmission electron microscopy and atomic force microscopy revealed that thermal annealing enhanced the degree of aggregation of the CdSe tetrapods and induced denser morphologies, which enhanced the PCE of the device.

We used synchronized GIWAXS and GISAXS of enhanced spatial/time resolutions, we have captured the competing kinetics of PCBM aggregation and P3HT crystallization of the corresponding BHJ thin-film solar cells. Within the first 100 s of thermal annealing at $150 \text{ }^\circ\text{C}$, PCBM aggregation size in the P3HT/PCBM composite films grew quickly from 7 to 18 nm then saturated; meanwhile, the majority P3HT lamellae increased from a size of 7 to 12 nm. Both the kinetics of PCBM aggregation and P3HT crystallization could be characterized by similar Avrami exponents close to unity; the faster PCBM aggregation, however, has a 2-fold higher Avrami rate constant. The mutually confined growths led to comparable nanograin sizes of PCBM and P3HT below 20 nm, when annealing temperature was kept below $180 \text{ }^\circ\text{C}$. The developments of PCBM and P3HT nanodomains could influence strongly and sensitively the electron and hole mobilities of the BHJ thin-film solar cells. The illustrated kinetics of structural evolution and its correlation to changes in charge mobility of P3HT/PCBM composite films may bear relevance to the selection of alternative polymer/fullerene derivative combinations and in the optimization of processing conditions for future BHJ thin-film solar cells.

Keywords: conducting conjugated polymer, polymer solar cell, CdSe, PbSe QDs, thermal annealing, crystalline kinetics

摘要

在這項研究中，我們用一層聚(3,4- 乙烯基)：(苯乙烯磺酸鈉) (PEDOT:PSS) 電洞傳輸層，提升硒化鉛量子點 (QD) 太陽能電池元件在AM1.5 標準頻譜下之光電轉換效率，從標準的硒化鉛量子點元件，效率由 1.5% 提升至 2.4%。利用同步輻射 X 射線反射測量顯示，各層之間的界面的粗糙度因存在的 PEDOT:PSS 層而急劇下降。此外，根據連續模擬 AM1.5 照射 ($100\text{mW}/\text{CM}^2$) 元件的壽命時間，我們發現硒化鉛量子點結合的 PEDOT:PSS 薄膜元件在降低效率到原先的 80% 所需的時間是 6 倍以上的標準硒化鉛量子點元件。(*Advanced Functional Materials*, **2010**, 20, 3555-3560)

我們已經使用了 Stille 聚合準備噻吩並 [3,4 - C] 吡咯- 4,6 - 二酮 (TPD) 基聚合物 PBTTTPD，具有優良的熱穩定性，結晶的特點，和較低的 HOMO 能階; 這些理想的特性意味著 PBTTTPD 有潛力的聚合物太陽能電池的應用。通過元件結構與成分組成的優化製程，PBTTTPD / PCBM 太陽能電池元件 0.95V 的開路電壓，而整體的光電轉換效率為 4.7%。(*Macromolecules*, **2010**, 43, 6936-6938)

我們在量子點太陽能電池元件的基礎上對 CdSe 四角錐狀和利用供體/受體的混摻膜結合共軛聚合物 PDTTTPD，其中包括 2,5 - 二(2 - 噻吩基) 噻吩並 [3,2 - b] 噻吩 噻吩並 [3,4 - C] 吡咯-4,6 - 二酮單位。在 AM1.5 標準量測環境下的光電轉換效率 (PCE) 在與 CdSe 四角錐狀/ PDTTTPD 的混合比為 1:9，W/W 的元件是 PDTTTPD/ 硒化鎘四角錐狀具有 1:1，W/W 混合 (2.9% 與 1.0%) 的三倍。同步輻射 X 射線反射顯示，退火造成 PDTTTPD/ 硒化鎘四角錐狀共混膜的減少相對的元件膜厚度。穿透式電子顯微鏡和原子力顯微鏡發現，熱退火的 CdSe 四角錐狀和形態的聚集程度會因退火而增強，導致大幅增加元件效率。(*Energy Environ. Sci.*, **2011**, 4, 2316-2322)

我們使用同步 GIWAXS/GISAXS 在即時同步調件下之分辨技術，我們已獲知 PCBM 聚集和相應的塊狀異質界面高分子太陽能電池的 P3HT 結晶動力學。PCBM 聚集的大小在 P3HT/PCBM 複合薄膜於熱退火 150°C 的條件下，從 7 奈米提升至 18 奈米，然後飽和迅速增長在 100 秒時間內，同時，多數 P3HT 與片狀大小，從 7 奈米增大至 12 奈米的大小。PCBM 聚集和 P3HT 結晶的動力學可利用特徵相似的 Avrami 指數近似逼近分析; 我們發現更快 PCBM 聚集，有一個高 2 倍 Avrami 速率常數。相互密閉的增長導致可使 PCBM 和 P3HT 具有 20 奈米以下的奈米晶的大小，當退火溫度低於 180°C 下保持 PCBM 和 P3HT 奈米區塊的發展可能會強烈影響塊狀異質界面高分子太陽能電池的電子和電洞遷移率。元件構造在熱火的製程中 P3HT/PCBM 膜的流動性的變化說明了動力學可能承擔相關的替代聚合物/富勒烯衍生物的組合選擇，並可在未來高分子太陽能電池的製程條件做出相關的貢獻。(*ACS Nano*, **2011**, 5, 6233-6243)

關鍵字: 共軛導電高分子、高分子太陽能電池、硒化鎘、硒化鉛量子點、熱退火、結晶動力學

Introduction

The development of conjugated polymers for use in organic optoelectronic devices is an active field of research. In particular, polymer heterojunction solar cells have attracted much attention because of their potential application in large-area, flexible, low-cost devices^[1,2]. The power conversion efficiencies (PCEs) of bulk heterojunction (BHJ) solar cells have improved dramatically over the last few years. For example, the PCEs of BHJ solar cells, incorporating regioregular poly(3-hexylthiophene) (P3HT) as the donor and [6,6]-phenyl-C61-butyric acid methyl ester (PCBM) as the acceptor, have recently reached values of ca. 4–5% under standard solar conditions (AM 1.5 G, 100 mW cm⁻²) [3]. Nevertheless, the PCEs of these polymer BHJ devices must improve further if they are to be employed practically, necessitating the development of unconventional structures.

Fabricating photovoltaic devices using solution-processed materials has many potential benefits, particularly for the rapid and economical preparation of flexible, large-area devices. Solution processing of organic polymers, inorganic semiconductors, and organic/inorganic hybrids has been adopted widely. One example of the use of conjugated polymers is in the preparation of heterojunction photovoltaic devices, which have achieved solar conversion efficiencies greater than 7%. Nevertheless, because composites of low-bandgap conjugated polymers and fullerene derivatives remain active only at wavelengths from 300 to 800 nm, they fail to harvest most of the radiation in the infrared (IR) spectral region. By virtue of the quantum size effect, colloidal quantum dots (QDs) of Pb salts have absorption characteristics that can be tuned throughout the IR spectrum.

Here, we have prepared photovoltaic devices featuring a PEDOT:PSS hole transport layer and three individually deposited PbSe QD layers. The PbSe photovoltaic devices incorporating the PEDOT:PSS layer exhibited enhanced AM1.5 PCEs relative to those of devices lacking the hole transport layer, with an enhancement factor of 60%. The roughness of the interface between the PEDOT:PSS and PbSe QD layers was almost three times less than that of the original ITO–PbSe QD interface, as measured using X-ray reflectivity. Hence, the presence of the PEDOT:PSS layer not only provided a smoother interface between the PbSe QD layers and the ITO substrate but also resulted in enhanced open-circuit voltages. In addition, the presence of the PEDOT:PSS hole transport layer prolonged the life time, as measured in terms of the time required to reach 80% of the normalized efficiency, of the PbSe QD solar device by six-fold, suggesting that this approach improves the performance of PbSe QD photovoltaic devices.

Novel donor-acceptor conjugated polymer, conjugated polymers featuring electron donor and acceptor (D–A) units in their main and/or side chains are quite attractive because of their tunable electronic properties, ambipolar charge transport abilities, and enlarged spectral absorption ranges.[4,5] In this study, we have used Stille polymerization to prepare the thieno[3,4-c]pyrrole-4,6-dione (TPD)-based polymer PBTTPD, which features excellent thermal stability, crystalline characteristics, and a low-lying HOMO energy level; these desirable properties mean that PBTTPD has promising potential for application in polymer solar cells. Through devices' composition optimization, a device incorporating the PBTTPD/PCBM blend at a weight ratio of 1:1.5 displayed an open-circuit voltage of 0.95 V and, therefore, a PCE of 4.7%.

The development of composite materials comprising a conjugated polymer as the hole acceptor and a solution-processable inorganic semiconductor nanocrystal as the electron acceptor for use in BHJ photovoltaic systems has recently undergone several major advances. For example, conjugated polymer/nanocrystal

photovoltaic devices containing CdSe nanocrystals (one of the most investigated materials for use as the electron acceptor), fabricated in combination with poly-(3-hexylthiophene) (P3HT),^{18–21} OC1C10 PPV,^{22,23} MEH-PPV,²⁴ and the alternating polyfluorene copolymer APFO-325 as hole acceptors, have exhibited AM1.5G power conversion efficiencies (PCEs) in the range 1.4–2.6%. Moreover, large improvements in PCEs (up to 3.1%) have been obtained when combining CdSe tetrapods with poly[2,6-(4,4-bis-(2-ethylhexyl)-4H-cyclopenta[2,1-b;3,4-b']-dithiophene)-alt-4,7-(2,1,3-benzothiadiazole)](PCPDTBT).^[6]

In principle, photovoltaic devices should exhibit excellent performance when incorporating polymer/CdSe tetrapods in the BHJ not only because of the high absorption coefficient and tunable band gap of CdSe nanocrystals, but also its shape is optimal arrangement for electron extraction. The electron-deficient thieno[3,4-c]pyrrole-4,6-dione (TPD) moiety exhibits asymmetric, rigidly fused, coplanar structure with strong electron withdrawing properties, making it a potentially useful system for increasing the strength and number of intramolecular/intermolecular interactions and lowering the highest occupied molecular orbital (HOMO) energy levels when incorporated into polymeric backbones, resulting in enhanced open-circuit voltages (V_{oc}) in BHJ solar cells.^[7,8]

Morphology of the active layer of bulk heterojunction (BHJ) thin films, comprising donor and acceptor components, is one of the critical factors in solar cell performance optimization. An ideal morphology for BHJ thin-film solar cells features in phase-separated nanodomains ca. 10 nm in size to facilitate exciton dissociation and charge transport; also relevant is the connectivity of these nanodomains in the respective phases for charge transport. In the past decade, BHJ thin film processing parameters, such as composition, annealing temperature/time, casting solvent, and film thickness, have been intensively studied. As a result, power conversion efficiency (PCE) in excess of 4% could be obtained with the popular BHJ blend of regioregular poly(3-hexylthiophene) (P3HT) and [6,6]-phenyl-C61-butyric acid methyl ester (PCBM). In general, optimized device performance of this BHJ blend can be achieved with films of PCBM/P3HT weight ratio $c = 0.8\sim 1.0$ and ca. 100 nm in thickness after thermal annealing at 120~160°C for 15~30 min; processing details determine that these parameters fluctuate in a certain range.

Results and Discussion

Figure 1 displays the current density–voltage characteristics of a device incorporating a 95-nm-thick layer of 4.5-nm-diameter PbSe QDs under AM 1.5G conditions (100 mW cm^{-2} , 25°C) and in the dark. **Figure 1** displays the energy band diagram for the various layers in the device. The value of J_{sc} increased to 21.9 mA cm^{-2} for the device incorporating the PEDOT:PSS layer from 18.0 mA cm^{-2} for the unmodified device, an increase of ca. 20%, presumably because of superior interfacial contacts and, therefore, improved carrier transport between the PbSe QDs and the PEDOT:PSS layer. The fill factors (FFs) of these two devices, however, were similar. **Table 1** lists the current density–voltage characteristics of the PbSe QD device, incorporating a PEDOT:PSS intermediate layer, under 100 mW cm^{-2} solar AM1.5G illumination. **Figure 2 a** presents a cross-sectional TEM image of a device incorporating a PEDOT:PSS layer (thickness: 20 nm) and a PbSe QD active layer (thickness: $95 \pm 5 \text{ nm}$); two interfaces are clearly evident in the active layer (i.e., PbSe-1–PbSe-2 and PbSe-2–PbSe-3).

Figure 2 b presents XRR curves of the PbSe QD films on ITO substrates, in the presence and absence of the PEDOT:PSS layer. The curve of the device incorporating the PEDOT:PSS layer exhibits oscillating behavior between 0.3 and 1.0 nm^{-1} ; that of the device lacking a PEDOT:PSS layer appears to be deprived such features, providing further evidence that the presence of the PEDOT:PSS layer results in a reduction of the interfaces roughness in the device since the physical smoothness of the interface between layers is inversely proportional to the smoothness of its X-ray reflectivity curve. **Figure 3** reveals that the stability of the PCE of the device incorporating the PEDOT:PSS layer was substantially greater relative to that of the device lacking the PEDOT:PSS layer. In particular, the device life times, measured in terms of the time required to reach 80% of the normalized efficiency, for the standard PbSe QD device and the PbSe QD device incorporating the PEDOT:PSS layer were 20 and 120 min, respectively, a six-fold improvement for the latter. Notably, the device incorporating the PEDOT:PSS layer exhibited almost constant values of J_{sc} and FF during its first 60 min of operation; in contrast, its value of V_{oc} decreased gradually. Since the incorporation of PEDOT:PSS layer in the device can result in the smoothening of the interfaces between various layers, the packing of PbSe QDs therefore becomes better, and possibly less defects and cracks were introduced in the device structure, relative to that of the device lacking the PEDOT:PSS layer. Consequently, under continuous illumination the degradation in the V_{oc} of the device with PEDOT:PSS layer slows down, which in turn mitigates the degradation of the PCE of the device.

We prepared PBTPD (**Scheme 1**) through Stille polymerization of the monomers 1,3-dibromo-5-ethylhexylthieno[3,4-c]pyrrole-4,6-dione (M1) and 4,40-didocecy-5,50-bis(trimethylstannyl)-2,20-bithiophene (M2) using tris(dibenzylideneacetone)dipalladium/tri-(*o*-tolyl)phosphine [Pd2dba3/P(*o*-tolyl)3] as the catalyst. The branched 2-ethylhexyl chain of the TPD moiety was present to promote the solubility of the polymer. The number-average molecular weight of PBTPD was 9.7 kg mol^{-1} , with a polydispersity of 1.4, as determined through gel permeation chromatography (GPC) using chloroform as the eluent. This polymer was readily soluble in hot chlorinated solvents, namely chloroform, chlorobenzene, and dichlorobenzene. PBTPD exhibited good thermal stability, with its decomposition temperature (T_d) greater than 400°C , as measured using thermogravimetric analysis.

In **Figure 4a**, the (100), (200), and (300) diffraction peaks for PBTPD are at 3.4° , 6.8° , and 10.2° ,

respectively, indicating a highly ordered structure along with a d-spacing of 26 anstrom that is ascribable to the interchain distance separated by the alkyl side chains; the broad feature at 24.6° , corresponding to a short distance of 3.6 anstrom, is assigned to the facial π - π stacking between polymeric backbones; such high crystallinity suggested that PBTTTPD would exhibit good carrier mobility when applied in PSCs. **Figure 4b** presents absorption spectra of PBTTTPD in dilute chloroform solution and in the solid state. In solution, the polymer exhibited an absorption signal at 468 nm, which we assign to internal charge transfer between the TPD acceptor and the bithiophene donor. The absorption maximum of the solid state polymer appeared at 572 nm; a significant red shift of 104 nm relative to that in solution, indicating that considerably strong intermolecular interactions existed in the solid film. Additionally, a vibronic shoulder at 628 nm implies an ordered arrangement of PBTTTPD in the solid film, with strong π - π stacking between the polymeric backbones, a feature that also appears in regioregular poly(3-hexylthiophene). **Figure 5** presents the current density-voltage curves of the BHJ solar cells with different active layer compositions in the dark and under the illumination; **Table 2** summarizes the data. The optimal device efficiency was obtained from the device with an active layer that comprised a blend of PBTTTPD and PCBM at a weight ratio of 1:1.5; this device displayed a value of V_{oc} of 0.95 V, a short-circuit current density (J_{sc}) of 8.02 mA cm^{-2} , a fill factor of 0.62, and a resulting PCE of 4.7%.

Figure 6a presents the optical absorption spectra of spin-coated films of the pyridine-treated CdSe tetrapods, the pure PDTTTPD, and the PDTTTPD/CdSe (1 : 9, w/w) blend. The thin film of the pyridine-treated CdSe tetrapods exhibits its first absorption peak at 630 nm and a strong absorbance in the shorter wavelength region between 350 and 550 nm, complementing the inferior absorption of the polymers in this region. In the spectrum of the PDTTTPD thin film, we assign the absorption maximum at 510 nm to intramolecular charge transfer between the DTT donor and TPD acceptor. In addition, a vibronic shoulder appeared at 620 nm in the spectrum, attributable to ordered molecular arrangement during the precipitation process. The spectrum of the composite film appears as a superposition of the respective absorption spectra of the pure PDTTTPD and CdSe components; therefore, no electronic interaction occurred between the PDTTTPD polymer strands and the CdSe tetrapods. **Figure 6b** displays the architecture of a fabricated photovoltaic device having the sandwich structure indium tin oxide (ITO)/poly-(3,4-ethylenedioxythiophene):polystyrenesulfonate (PEDOT:PSS)/PDTTTPD:CdSe tetrapods (1 : 9, w/w)/Al.

Figure 7 displays the current density-voltage characteristics of the photovoltaic devices incorporating PDTTTPD/CdSe (1 : 9, w/w) active layers that had been subjected to thermal annealing at 130°C for 10–30 min. Measurements were performed under AM1.5G illumination (100 mW cm^{-2}) in a N_2 -filled glove box. The thickness of the active layer in each of these devices was $130 \pm 20 \text{ nm}$. Table 1 lists the short-circuit current densities (J_{sc}), values of V_{oc} , fill factors (FFs), and PCEs of these heterojunction PDTTTPD–CdSe photovoltaic devices. The values of V_{oc} for these blend devices were in the range 0.88–0.89 V, with only slight differences arising from the different annealing times. The values of J_{sc} and FF of the PDTTTPD/CdSe blend devices after annealing treatment were significantly higher than those of the as-prepared blend device. Because annealing of the PDTTTPD/CdSe tetrapod film caused the thickness of the film to decrease from 150 nm to 135 nm, with an associated increase in the film density. Therefore, removal of pyridine ligands from the CdSe tetrapods decreased the interparticle distance and, in turn, increased the CdSe tetrapods' packing densities, thereby improving the conductivity in the active layer.

With the experimental setup shown in **Figure 8**, we could measure time resolved GIWAXS and GISAXS

patterns simultaneously for the P3HT/PCBM composite films ($c = 1.0$) in situ annealed at 150°C .

Figure 9a presents the GISAXS profiles of the P3HT/PCBM ($c = 1.0$) film selectively extracted from the corresponding 2D patterns along the qx direction (at the specular beam position $qz \approx 0.018 \text{ \AA}^{-1}$), revealing the fast scattering development in the low- q region $0.004\sim 0.04 \text{ \AA}^{-1}$ within the first 60 s of thermal annealing. Furthermore, the selected GISAXS profiles (**Figure 9c**) for 60, 600, and 1800 s at 150°C overlapped roughly, revealing quickly saturated PCBM aggregation. A broad interference shoulder at $qx \approx 0.025 \text{ \AA}^{-1}$ shaped during the annealing, corresponding to formation of a liquid-like or distorted face-centered-cubic-like packing of PCBM aggregates with a mean spacing of ca. 25 nm (detailed below with model fitting). For comparison, the GISAXS profile similarly measured for a pristine P3HT film annealed at 150°C for 1800 s contributed only marginally in this monitored q region, as illustrated in **Figure 9c**. Shown in **Figure 9b,d** are the size distributions (in general, 20~30%) and the size evolution during annealing, indicating that PCBM aggregates grew slightly from a diameter of ca. 7 nm (as-cast film) to 10 nm during heating toward 150°C . In the subsequent 60 s of isothermal annealing, the PCBM aggregate size increased quickly from 10 to 17.5 nm, then remained about the same in the prolonged thermal annealing over 1800 s. In all of the GISAXS data fitting, we had to include a scattering term described by the Debye-Buche correlation function, $I(qx) = (1 + qx^2\zeta^2)^{-2}$, to account for the relatively sharp upturn scattering in the very low- q region $0.004\sim 0.007 \text{ \AA}^{-1}$. The fitted values for the Debye-Buche correlation length ζ were about the same (10 nm) for all sets of data; hence, the structural origin of this correlation length might be irrelevant to PCBM aggregation. Possibly, the correlation length might associate better with the reported P3HT aggregates of nanowhisker or protofibril structure already formed in solutions.

To correlate the morphological development of the P3HT/PCBM thin films to the corresponding solar cell performance, we have further monitored the changes of electron and hole mobilities for a BHJ film with $c = 1.0$ during annealing at 150°C . Shown in Figure 8a is the uprising electron mobility, μ_e , observed within the first 100 s of thermal annealing, which becomes saturated subsequently. This synchronizes well with the development of $R(t)$ for the PCBM aggregation (**Figure 10a**). Similarly observed is the accompanied development of the hole mobility, μ_h , that saturated slightly later than the electron mobility (**Figure 10b**). Correspondingly, the development of hole mobility synchronized with the $R(t)$ for the development of P3HT lamellae, as illustrated in **Figure 10b**. These sensitive responses indicate that charge mobilities in the BHJ solar cell and consequently the short-circuit current density J_{sc} depend strongly on the developments of the P3HT and PCBM nanodomains upon heat treatment, whereas the increase of optical absorption owing to enhanced P3HT crystallization observed previously contributes only partly to J_{sc} . Note that the values of the electron and hole mobilities obtained might be subject to device preparation conditions to some extent, and we believe that the relative values, hence the growth trends, of the charge mobilities shown in **Figure 10** should be reliable. The bulk structural characteristics extracted from GISAXS/GIWAXS for the P3HT/PCBM thin-film solar cells annealed at various temperatures are correlated to the corresponding device performance parameters extracted, with the corresponding current density-voltage curves; accordingly, a cartoon in **Figure 11** depicts the morphological features. Interestingly, the structure model is very much in line with the predictions based on the temperature-composition phase diagram of the binary P3HT-PCBM blend previously given by Kim and Frisbie, in that below 200°C and within the concentration range of 30~50 wt % (or $c = 0.5\sim 1.0$), PCBM is expected to dissolve in P3HT, in the form of dispersed molecules or noncrystalline aggregates, forming a metastable phase.

Conclusions

We have prepared photovoltaic devices featuring a PEDOT:PSS hole transport layer and three individually deposited PbSe QD layers. The PbSe photovoltaic devices incorporating the PEDOT:PSS layer exhibited enhanced AM1.5 PCEs relative to those of devices lacking the hole transport layer, with an enhancement factor of 60%. The roughness of the interface between the PEDOT:PSS and PbSe QD layers was almost three times less than that of the original ITO–PbSe QD interface, as measured using X-ray reflectivity. Hence, the presence of the PEDOT:PSS layer not only provided a smoother interface between the PbSe QD layers and the ITO substrate but also resulted in enhanced open-circuit voltages. In addition, the presence of the PEDOT:PSS hole transport layer prolonged the life time, as measured in terms of the time required to reach 80% of the normalized efficiency, of the PbSe QD solar device by six-fold, suggesting that this approach improves the performance of PbSe QD photovoltaic devices.

We have used Stille polymerization to prepare the thieno[3,4-c]pyrrole-4,6-dione (TPD)-based polymer PBTTTPD, which features excellent thermal stability, crystalline characteristics, and a low-lying HOMO energy level; these desirable properties mean that PBTTTPD has promising potential for application in polymer solar cells. Through devices' composition optimization, a device incorporating the PBTTTPD/PCBM blend at a weight ratio of 1:1.5 displayed an open-circuit voltage of 0.95 V and, therefore, a PCE of 4.7%.

We have prepared BHJ photovoltaic devices based on PDTTTPD and CdSe tetrapods and optimized their PCE through annealing treatment. In particular, annealing of devices incorporating PDTTTPD/CdSe tetrapod blends (1 : 9, w/w) at 130°C for 20 min greatly enhanced the AM1.5 PCEs relative to those of the as-prepared blend devices, with an enhancement factor of three. This enhancement resulted from a sharp increase in the short-circuit current density of the device, which contained a more-dense active layer and more highly aggregated CdSe tetrapods after thermal annealing, resulting from the much lower level of pyridine ligands on the CdSe tetrapods. Therefore, the annealing process played an important role in improving the device performance and morphology.

With synchronized GIWAXS and GISAXS of enhanced spatial/time resolutions, we have captured the competing kinetics of PCBM aggregation and P3HT crystallization of the corresponding BHJ thin-film solar cells. Within the first 100 s of thermal annealing at 150 °C, PCBM aggregation size in the P3HT/PCBM composite films grew quickly from 7 to 18 nm then saturated; meanwhile, the majority P3HT lamellae increased from a size of 7 to 12 nm. Both the kinetics of PCBM aggregation and P3HT crystallization could be characterized by similar Avrami exponents close to unity; the faster PCBM aggregation, however, has a 2-fold higher Avrami rate constant. The mutually confined growths led to comparable nanograin sizes of PCBM and P3HT below 20 nm, when annealing temperature was kept below 180 °C. The developments of PCBM and P3HT nanodomains could influence strongly and sensitively the electron and hole mobilities of the BHJ thin-film solar cells. The illustrated kinetics of structural evolution and its correlation to changes in charge mobility of P3HT/PCBM composite films may bear relevance to the selection of alternative polymer/fullerene derivative combinations and in the optimization of processing conditions for future BHJ thin-film solar cells.

References

- [1] G. Yu, J. Gao, J. C. Hummelen, F. Wudl and A. J. Heeger, **1995** *Science* 270 1789
- [2] S. H. Park, A. Roy, S. Beaupre, S. Cho, N. Coates, J. S. Moon, D. Moses, M. Leclerc, K. Lee and A. J.

Heeger **2009** *Nat. Photon.* 3 297

[3] Li G, Shrotriya V, Huang J, Yao Y, Moriarty T, Emery K and Yang Y **2005** *Nat. Mater.* 4 864.

[4] A. Gadisa, W. Mammo, L. M. Andersson, S. Admassie, F. L. Zhang, M. R. Andersson, O. Inganas, *Adv. Funct. Mater.* **2007**, 17, 3836.

[5] Y. Liang, D. Feng, Y. Wu, S. T. Tsai, G. Li, C. Ray, L. Yu, *J. Am. Chem. Soc.* **2009**, 131, 7792.

[6] S. Dayal, N. Kopidakis, D. C. Olson, D. S. Ginley and G. Rumbles, *Nano Lett.*, **2010**, 10, 239.

[7] C. Piliago, T. W. Holcombe, J. D. Douglas, C. H. Woo, P. M. Beaujuge and J. M. J. Fréchet, *J. Am. Chem. Soc.*, **2010**, 132, 7595.

[8] A. Najari, S. Beauprê, P. Berrouard, Y. Zou, J. R. Pouliot, C. L. P. _erusse and M. Leclerc, *Adv. Funct. Mater.*, **2010**, 21, 718.

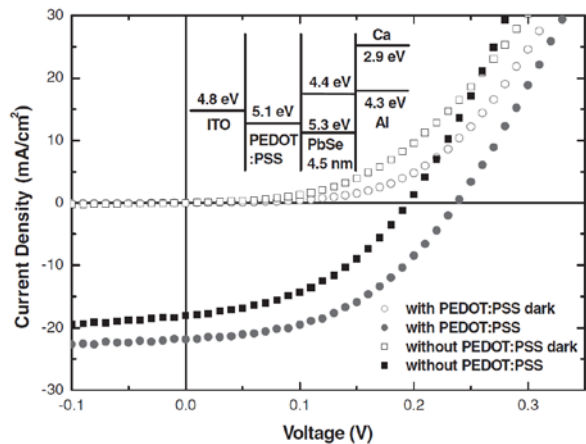


Figure 1. Current density–voltage characteristics of 4.5-nm-diameter PbSe QD devices incorporating a PEDOT:PSS intermediate layer, recorded in the dark and under solar illumination (100 mW cm^{-2}). Inset: Energy-level diagram for a PbSe QD photovoltaic device.

Table 1. Performance parameters of PbSe QD devices incorporating a PEDOT:PSS intermediate layer, under solar illumination.

Device structure	V_{oc} [V]	J_{sc} [mA cm^{-2}]	FF [%]	η [%] [a]
ITO/PbSe/Ca/Al	0.19	18.0	44.0	1.5
ITO/PEDOT:PSS/PbSe/Ca/Al	0.24	21.9	45.5	2.4

[a] η : PCE. Solar: AM1.5G (100 mW cm^{-2}).

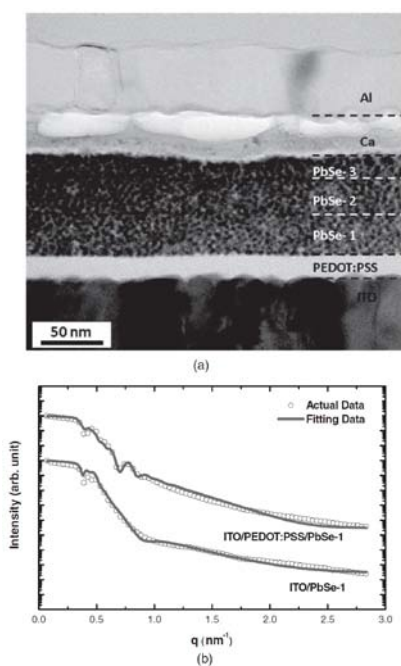


Figure 2. a) TEM cross-sectional image of the ITO/PEDOT:PSS/PbSe QD film/Ca/Al device stack; scale bar: 50 nm. b) Synchrotron X-ray reflectance for structures incorporating PbSe QD layers, prepared with and without a PEDOT:PSS thin layer.

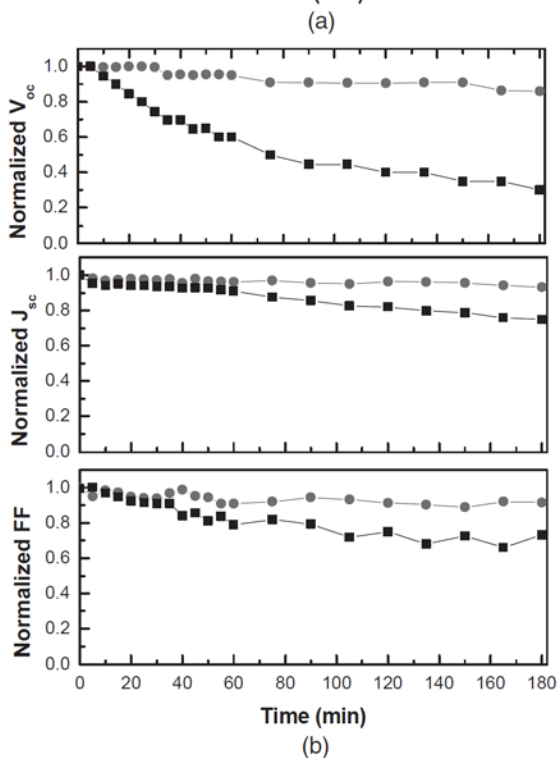
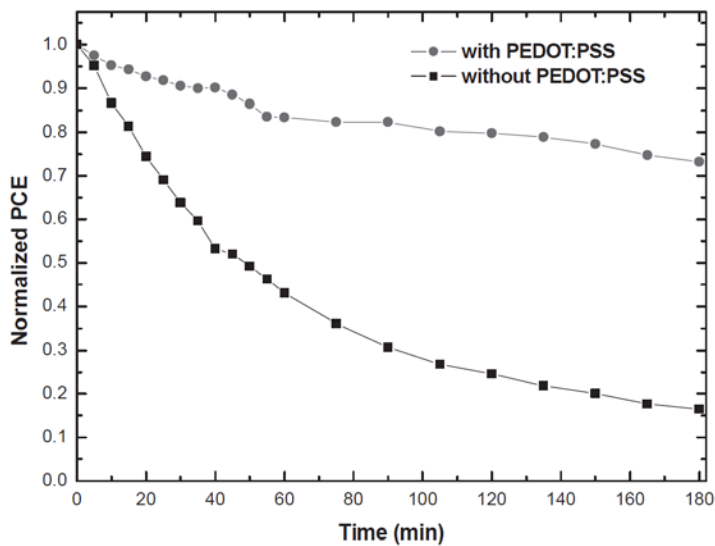
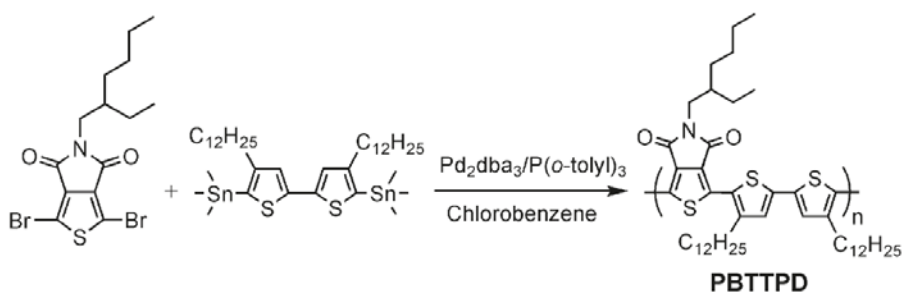


Figure 3. Values of **a)** PCE, **b)** V_{oc} , J_{sc} , and FF, measured as a function of time and normalized with respect to their initially measured values, for devices prepared with and without a PEDOT:PSS intermediate layer, illuminated continuously under simulated AM1.5G irradiation (100 mW cm^{-2}).

Scheme 1. Synthetic Route and Structure of PBTPD



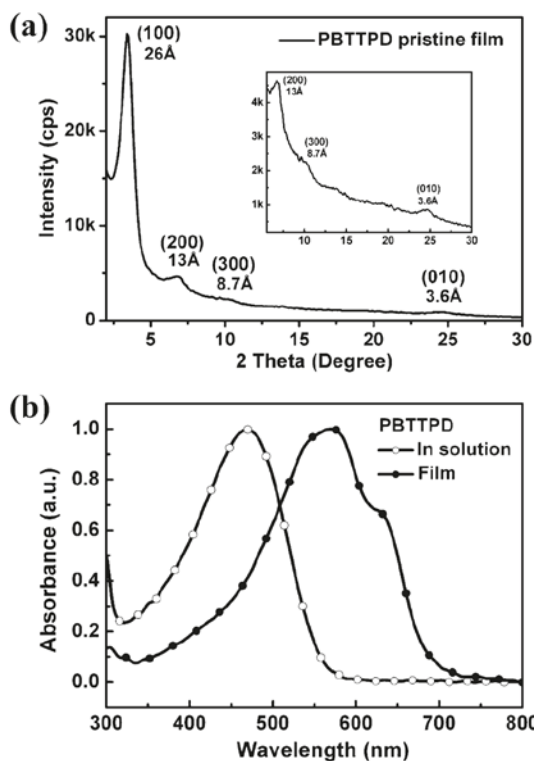


Figure 4. (a) X-ray diffraction pattern of the pristine PBTPPD film. (b) UV-vis absorption spectra of PBTPPD in dilute CHCl_3 and as a solid film.

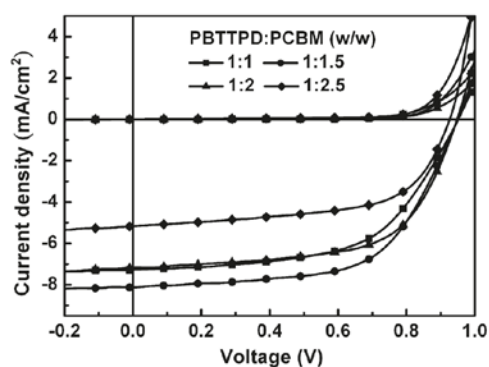


Figure 5. Current density-voltage (J-V) characteristics of PSCs incorporating the PBTPPD:PCBM blend at various weight ratios (w/w).

Table 2. Photovoltaic Properties of Polymer Solar Cells Incorporating PBTPPD:PCBM Blends Prepared at Various Weight Ratios

ratio (w/w)	V_{oc} (V)	J_{sc} (mA cm^{-2})	FF	PCE (%)
1:1	0.95	7.23	58	4.0
1:1.5	0.95	8.02	62	4.7
1:2	0.95	7.16	63	4.3
1:2.5	0.93	5.12	61	2.9

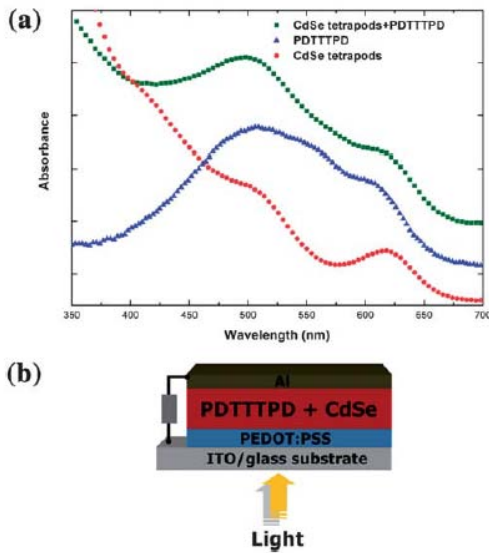


Figure 6 (a) Optical absorption spectra for spin-coated films of pure PDTTTPD (triangles), pure CdSe tetrapods (circles), and the PDTTTPD/CdSe tetrapod blend (squares). (b) Schematic structure of a PDTTTPD/CdSe tetrapod photovoltaic device.

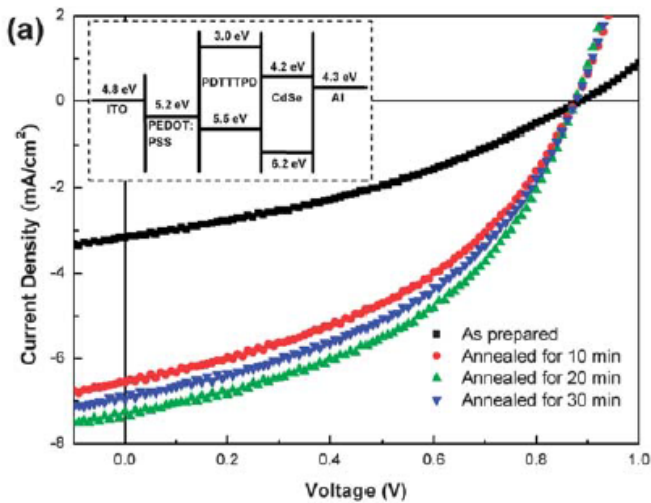


Figure 7 Current density–voltage characteristics (inset: energy level diagram)

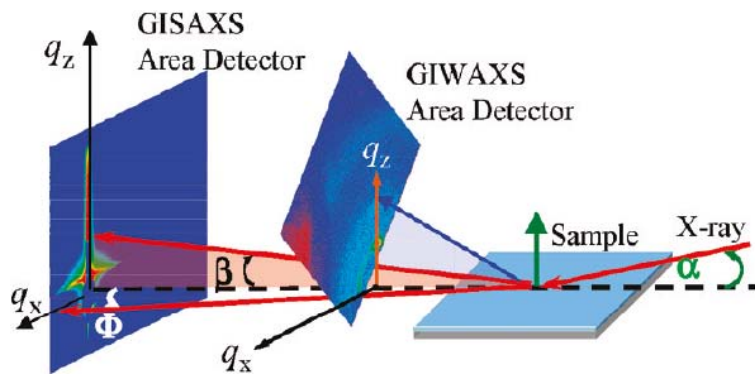


Figure 8. Schematic of the setup for synchronized GISAXS/ GIWAXS, with the beam incident angle R and the scattering angles β and Φ in the out-of-plane (q_z) and in-plane directions (q_x). The GIWAXS detector plane was normal to the incident beam; the detector was tilted 45° out of the horizontal plane to cover

scattering in the q_z and q_x directions.

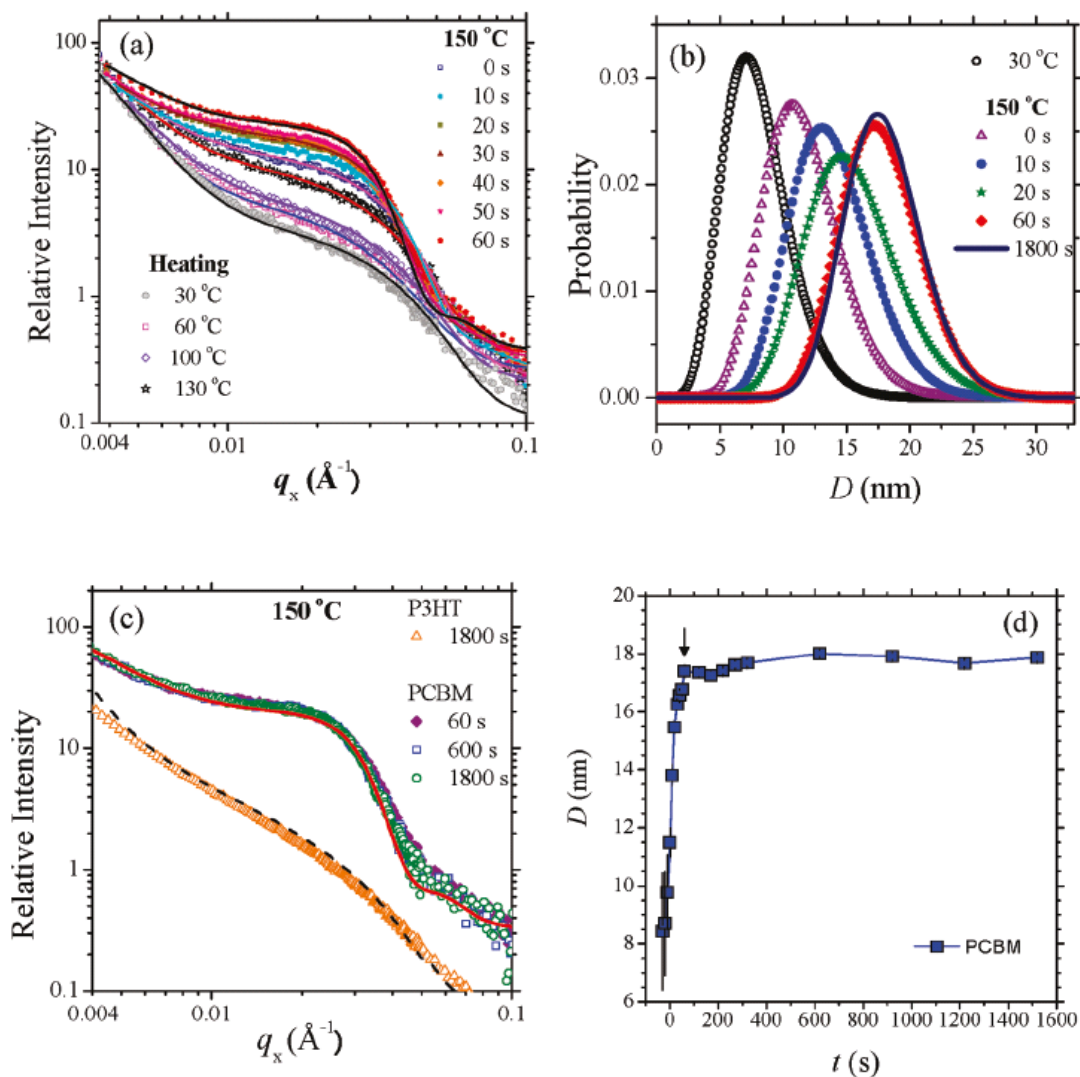


Figure 9. (a) Selected GISAXS profiles measured for the P3HT/PCBM film ($c = 1.0$) during the heating process to 150°C and the subsequent isothermal annealing within 60 s. The data are fitted (solid curves) using polydisperse spheres with the Schultz size distributions shown in (b). (c) Approximately overlapped GISAXS data collected after 60, 600, and 1800 s of thermal annealing. The data for 1800 s are fitted (solid curve) with the size distribution shown in (b). For comparison, the GISAXS data for a pristine P3HT film annealed at 150°C for 1800 s are also shown; the data are fitted (dashed curve) with polydisperse (in rod length) rods. (d). Corresponding mean size (D) evolution of PCBM aggregates.

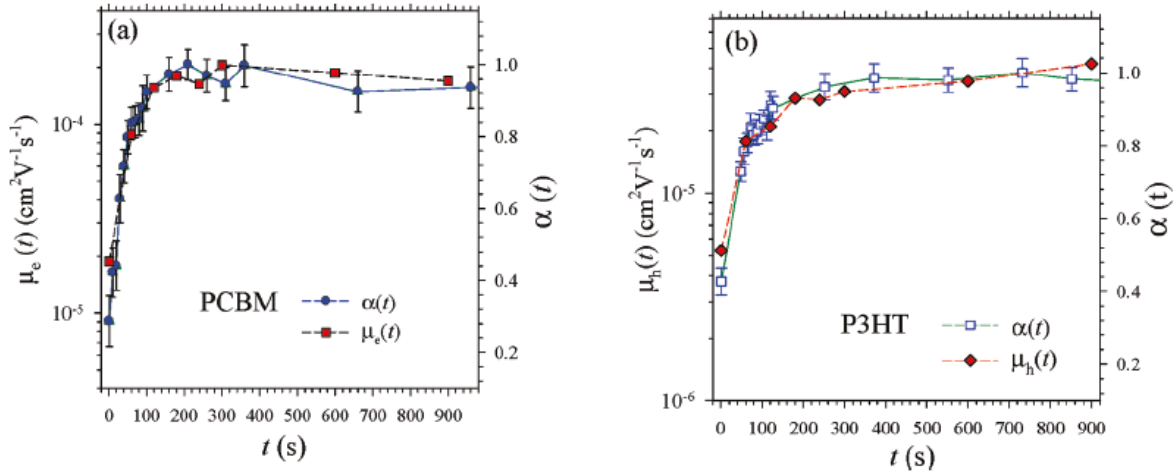


Figure 10. Strongly correlated developments of (a) the electron mobility and $R(t)$ of PCBM aggregation, and (b) the hole mobility and $R(t)$ of P3HT lamellae, of P3HT/PCBM composite films ($c = 1.0$) at 150°C annealing.

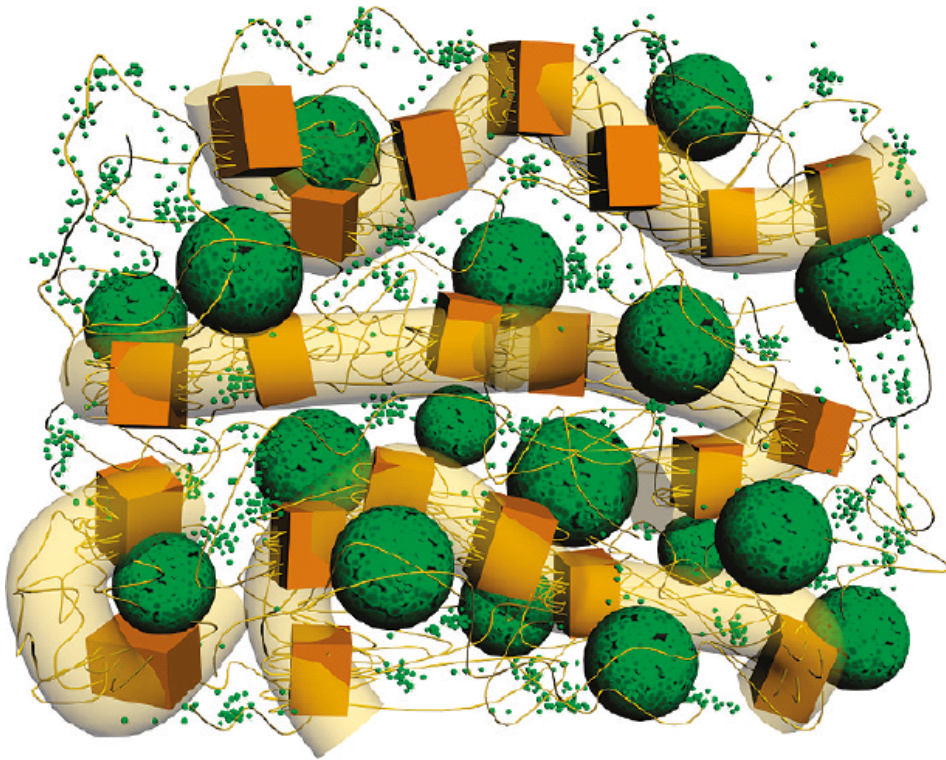


Figure 11. Cartoon for a thermally annealed P3HT/PCBM film, according to the structure characteristics shown in Table 3 (150°C case). The intercalated PCBM aggregates (large spheres) and P3HT crystallites (blocks) are immersed in the matrix of P3HT amorphous chains (thin wires) and dispersed PCBM molecules (small spheres).

國科會補助專題研究計畫成果報告自評表

請就研究內容與原計畫相符程度、達成預期目標情況、研究成果之學術或應用價值（簡要敘述成果所代表之意義、價值、影響或進一步發展之可能性）、是否適合在學術期刊發表或申請專利、主要發現或其他有關價值等，作一綜合評估。

1. 請就研究內容與原計畫相符程度、達成預期目標情況作一綜合評估

達成目標

未達成目標（請說明，以 100 字為限）

實驗失敗

因故實驗中斷

其他原因

說明：

2. 研究成果在學術期刊發表或申請專利等情形：

論文： 已發表 未發表之文稿 撰寫中 無

專利： 已獲得 申請中 無

技轉： 已技轉 洽談中 無

其他：（以 100 字為限）

3. 請依學術成就、技術創新、社會影響等方面，評估研究成果之學術或應用價值（簡要敘述成果所代表之意義、價值、影響或進一步發展之可能性）（以500字為限）

除了元件奈米結構的分析外，我們也著重於材料的開發，近幾年，元件內部奈米結構的分析已被世界各大研究團隊進一步提出許多分析的結果，但高分子與奈米碳球的能階排列分佈對元件效率也有極大的影響，先前我們是第一個提出主側、鏈予體受體共軛高分子的團隊(發表於 *Advanced Materials* **2009**, *21*, 2093–2097)，隨後研究主鏈予體受體之高結晶性共軛高分子應用於太陽能電池元件效率的差異性(發表於 *Macromolecules*, **2010**, *43*, 6936–6938)，此結果與美國加州大學柏克萊分校 Jean M. J. Freche 團隊得到的結果一致(*J. Am. Chem. Soc.*, **2010**, *132*, 7595–7597)，但是我們提出的高結晶性共軛高分子具有更高的開路電壓以及共軛高分子自身強烈的排列組裝，目前也已經進一步把效率提升到 6.15% 之境界(submitted to *Adv. Mater.* 2010)，並且未來可進一步應用在有機場效電晶體。

我們研究群在本奈米國家型科技計畫支助下產出之重大突破。在量子點元件奈米結構分析上，我們具體觀察到元件加入電洞傳輸層-聚(3,4-乙炔基二氧噻吩)/聚(苯乙烯磺酸鹽)對量子點堆疊的影響，未來在元件製程上此法可供元件製程開發的參考以提高元件效率，在新材料設計上，我們合成主鏈予體受體之高結晶性共軛高分子，元件開路電壓及效率有明顯提升。期望此新型高分子於未來在開發新穎材料與產業應用上建立良好基礎。

國科會補助計畫衍生研發成果推廣資料表

日期：__年__月__日

國科會補助計畫	計畫名稱：		
	計畫主持人：		
	計畫編號：	領域：	
研發成果名稱	(中文)		
	(英文)		
成果歸屬機構		發明人 (創作人)	
技術說明	(中文)		
	(200-500 字)		
	(英文)		
產業別			
技術/產品應用範圍			
技術移轉可行性及預期 效益			

註：本項研發成果若尚未申請專利，請勿揭露可申請專利之主要內容。

國科會補助專題研究計畫項下出席國際學術會議心得報告

日期：__年__月__日

計畫編號	NSC 99-2120-M-009-003 (99R445)		
計畫名稱	奈米結構異質接面高分子太陽能電池之材料開發及元件設計(3/3)		
出國人員姓名	韋光華	服務機構及職稱	交通大學材料所教授
會議時間	100年04月25日到100年04月29日	會議地點	美國加州舊金山
會議名稱	(中文)2011年美國材料學會(MRS)春季會議 (英文)2011 MRS Spring Meeting		
發表論文題目	(中文)溶劑致使高結晶性高分子與富勒烯炭球相分離效應運用在異質界面太陽能電池 (英文) Solvent Induced Phase-separated Morphology in Highly Crystalline Conjugated Polymer/fullerene Thin Films for Heterojunction.		

一、參加會議經過

本人本次參加2011年美國材料學會(MRS)春季之會議於4月24日晚上約八時搭機前往美國舊金山開會，於舊金山住於Marriott-Marquis Hotel，在在地機場遇到了清華大學洪銘輝教授及同步輻射中心李信義博士，三人於check in Hotel後晚上一起用餐。第二日(4月25日)即前往會議中心Moscone West註冊並領取會議資料及名牌。由於當日下午方開始有關高分子太陽能電池之報告，本人早上則於註冊後回Hotel準備第二日(4月26日)下午之受邀請之口頭報告、投影片。

本人於4月26日下午2時報告之題目為”Solvent Induced Phase-separated Morphology in Highly Crystalline Conjugated Polymer/fullerene Thin Films for Heterojunction.” 演講完時一共有4~5個問題顯示出聽眾用心聽講，當時共有2百多人在場。4月27日本人繼續聽了Steven Forrest, Yang Yang等人精彩之演講並與Yang Yang教授共進晚餐後，與洪銘輝教授一起前往機場搭深夜之長榮班機回台，並在舊金山機場遇到了清華大學陳力俊校長，陳校長此次前來參加接受美國材料學會會士之授予典禮。

二、與會心得

三、考察參觀活動(無是項活動者略)

四、建議

五、攜回資料名稱及內容

六、其他

國科會補助專題研究計畫項下出席國際學術會議心得報告

日期：__年__月__日

計畫編號	NSC 99-2120-M-009-003 (99R445)		
計畫名稱	奈米結構異質接面高分子太陽能電池之材料開發及元件設計(3/3)		
出國人員姓名	蘇明鑫 江建銘	服務機構及職稱	交通大學材料所博士班
會議時間	100年08月21日到100年08月25日	會議地點	美國加州聖地牙哥
會議名稱	(中文)國際光學工程學會-光電元件與應用 2011 (英文) SPIE Photonic Devices + Applications 2011		
發表論文題目	(中文)合成具苯並呋喃之高開路電壓共軛高分子並應用於有機高分子太陽能電池 溶劑致使高結晶性高分子與富勒烯炭球自我組裝效應運用在異質界面太陽能電池 (英文) High Open-Circuit Voltage Benzoxadiazole-Containing Polymers, Synthesis, Characterization and Photovoltaic Application. Solvent induced self-organization of crystalline conjugated polymer and fullerenes for heterojunction solar cells.		

一、參加會議經過

此次參加於美國加州聖地牙哥舉行之國際光學工程學會-光電元件與應用 2011 (SPIE Photonic Devices + Applications 2011)，於100年8月21日出發並於美國時間8

月 21 日星期日下午抵達飯店並且立即入住以後即先行前往會場確認會議議程。

美國時間 8 月 22 日星期一早上於十點抵達會場，並進行參加會議報到以及領取會議參加證件及相關文件，也一併把海報貼上所屬之欄位。當日下午便參予會議第一天之行程以及晚上海報展示與解說之活動，海報展示與解說之活動由下午 5 點半開始到 7 點半結束，於此活動以後便回到飯店結束此日之會議。

美國時間 8 月 23 日星期二，早上參加此趟會議之演講議程，此次分別有四個時段，其中演講者有美國史丹佛大學 Michael D. McGehee、美國國家再生能源實驗室(NREL)、韓國 Kwanghee Lee 教授、台灣大學林清富教授等，許多此領域知名學者與會，並且得到許多對研究有幫助的訊息。整個議程持續到當日下午 6 點結束。

美國時間 8 月 24 日星期三，早上 6 點便與飯店退房前往美國加州聖地牙哥國際機場搭乘回途班機。

二、與會心得

本次參與(SPIE Photonic Devices + Applications 2011)研討會在第一天海報展示及說明的過程中，與許多相同領域甚或不同領域之研究人員在實驗上的細節及數據上之分析互相交流，學習到許多不同的觀點及實驗手法，同時亦得知許多在光電領域上最新的知識及發展，對未來實驗方向及設計方面相信有良好之之助益。在議程演講的部分也有幸聆聽國際上此領域大師們的演講及他們實驗室的研究成果與發展，讓本人對實驗上的進一步發展與規劃有了新的認知與見解，也對未來的下一步看到許多新的可能性。與會後的心得主要在高分子太陽能電池的下一步發展，除了目前發展之低能隙高分子以期達到全波段吸光、增加光電流外，應該往較低之氧化能階方向設計，以降低高分子之 HOMO 能階，使其提高開路電壓並增加高分子之抗

氧化穩定性，提高壽命以及耐大氣環境的新穎材料發展，另外在高分子太陽能電池元件製作上，須輔以元件製程上的進步和元件內部形態分布的解析，才可以完整發揮新材料的本質特性，並往多層之元件結構設計，及反式元件製作法以達到完整使用材料的最大效益，並增加元件之存活時間與推展高分子太陽能電池的發展。

三、考察參觀活動(無是項活動者略)

四、建議

五、攜回資料名稱及內容

1. SPIE Photonic Devices + Applications 2011 Technical Program
2. SPIE Photonic Devices + Applications 2011 Exhibition Guide

六、其他

國科會補助專題研究計畫項下赴國外(或大陸地區)出差或研習心得報告

日期：__年__月__日

計畫編號	NSC 99-2120-M-009-003 (99R445)		
計畫名稱	奈米結構異質接面高分子太陽能電池之材料開發及元件設計(3/3)		
出國人員姓名	韋光華、劉志明、陳修成	服務機構及職稱	交通大學 材料系 教授與博士生
出國時間	100年10月26日至100年10月28日	出國地點	中國 武漢 華中科技大學

一、國外(大陸)研究過程

「太陽能電池課題研討會」

本人與博士生劉志明、陳修成於10月26日中午前往中國武漢參加「太陽能電池課題研討會」，並於10月26日晚上約六時抵中國之武漢國際機場，七時出關後即前往研討會之地點旁宏嘉酒店住宿，並進用晚餐。

第二天10月26日起研討會開始，首先為胡斌教授演說關於太陽能電池界面分析及討論，再來為韋光華教授演說關於太陽能電池有機高分子材料及討論，中午則與華中科技大學胡斌教授及山東大學解士傑教授共進中餐。下午則為解士傑教授演說關於太陽能電池光電轉換機制之理論計算及討論，以及參觀華中科技大學光電實驗室。第二天開始，上午8點30分即開始討論合作太陽能電池研究之相關細節，由本實驗室合成材料給華中大學做界面分析及理論計算，最後在十一時左右結束本研討會，用過午餐後於下午搭機回國。

二、研究成果

三、建議

四、其他

國科會補助專題研究計畫項下國際合作研究計畫國外研究報告

日期：__年__月__日

計畫編號	NSC — — — — —		
計畫名稱			
出國人員 姓名		服務機構 及職稱	
合作國家		合作機構	
出國時間	年 月 日至 年 月 日	出國地點	

一、國際合作研究過程

二、研究成果

三、建議

四、其他

赴國外研究心得報告

計畫編號	NSC 99-2120-M-009-003- (99R445)
計畫名稱	奈米結構異質接面高分子太陽能電池之材料開發及元件設計(3/3)
出國人員姓名 服務機關及職稱	韋光華、劉志明、陳修成 交通大學 材料系 教授
出國時間地點	October 26-28, 2011, 中國 武漢
國外研究機構	華中科技大學

工作記要：

「太陽能電池課題研討會」

本人與博士生劉志明、陳修成於10月26日中午前往中國武漢參加「太陽能電池課題研討會」，並於10月26日晚上約六時抵中國之武漢國際機場，七時出關後即前往研討會之地點旁宏嘉酒店住宿，並進用晚餐。

第二天10月26日起研討會開始，首先為胡斌教授演說關於太陽能電池界面分析及討論，再來為韋光華教授演說關於太陽能電池有機高分子材料及討論，中午則與華中科技大學胡斌教授及山東大學解士傑教授共進中餐。下午則為解士傑教授演說關於太陽能電池光電轉換機制之理論計算及討論，以及參觀華中科技大學光電實驗室。第二天開始，上午8點30分即開始討論合作太陽能電池研究之相關細節，由本實驗室合成材料給華中大學做界面分析及理論計算，最後在十一時左右結束本研討會，用過午餐後於下午搭機回國。

赴國外研究心得報告

計畫編號	NSC 99-2120-M-009-003 (99R445)
計畫名稱	奈米結構異質接面高分子太陽能電池之材料開發及元件設計(3/3)
出國人員姓名 服務機關及職稱	韋光華 交通大學 材料系 教授
出國時間地點	April 25-29, 2011 美國 舊金山
國外研究機構	美國材料學會 (Materials Research Society)
題目	Solvent Induced Phase-separated Morphology in Highly Crystalline Conjugated Polymer/fullerene Thin Films for Heterojunction.

工作記要：

本人本次參加 2011 年美國材料學會(MRS)春季之會議於 4 月 24 日晚上約八時搭機前往美國舊金山開會，於舊金山住於 Marriott-Marquis Hotel，在在地機場遇到了清華大學洪銘輝教授及同步輻射中心李信義博士，三人於 check in Hotel 後晚上一起用餐。第二日(4 月 25 日)即前往會議中心 Moscone West 註冊並領取會議資料及名牌。由於當日下午方開始有關高分子太陽能電池之報告，本人早上則於註冊後回 Hotel 準備第二日(4 月 26 日)下午之收邀請之口頭報告、投影片。

本人於 4 月 26 日下午 2 時報告之題目為” Solvent Induced Phase-separated Morphology in Highly Crystalline Conjugated Polymer/fullerene Thin Films for Heterojunction.” 演講完時一共有 4~5 個問題顯示出聽眾用心聽講，當時共有 2 百多人在場。4 月 27 日本人繼續聽了 Steven Forrest, Yang Yang 等人精彩之演講並與 Yang Yang 教授共進晚餐後，與洪銘輝教授一起前往機場搭深夜之長榮班機回台，並在舊金山機場遇到了清華大學陳力俊校長，陳校長此次前來參加接受美國材料學會會士之授予典禮。

國立交通大學博士班研究生

出席國際會議報告

報告人姓名	蘇明鑫	報告日期	100年08月31日
系所及年級	材料所 博士班五年級	核定文號	100年06月30日 11D117
連絡電話	03-5731771	電子信箱	redguest36.mse95g@nctu.edu.tw
會議期間	100年08月21日 到100年08月25日	會議地點	美國加州聖地牙哥
會議名稱	(中文) 國際光學工程學會-光電元件與應用 2011 (英文) SPIE Photonic Devices + Applications 2011		
發表論文題目	(中文) 溶劑致使高結晶性高分子與富勒烯炭球自我組裝效應運用在異質界面太陽能電池 (英文) Solvent induced self-organization of crystalline conjugated polymer and fullerenes for heterojunction solar cells		

報告內容包括下列各項：

一、 參加會議經過

此次參加於美國加州聖地牙哥舉行之國際光學工程學會-光電元件

與應用 2011 (SPIE Photonic Devices + Applications 2011)，於 100 年 8 月 21 日出發並於美國時間 8 月 21 日星期日下午抵達飯店並且立即入住以後即先行前往會場確認會議議程。

美國時間 8 月 22 日星期一早上於十點抵達會場，並進行參加會議報到以及領取會議參加證件及相關文件，也一併把海報貼上所屬之欄位。當日下午便參予會議第一天之行程以及晚上海報展示與解說之活動，海報展示與解說之活動由下午 5 點半開始到 7 點半結束，於此活動以後便回到飯店結束此日之會議。

美國時間 8 月 23 日星期二，早上參加此趟會議之演講議程，此次分別有四個時段，其中演講者有美國史丹佛大學 Michael D.

McGehee、美國國家再生能源實驗室(NREL)、韓國 Kwanghee Lee 教授、台灣大學林清富教授等，許多此領域知名學者與會，並且得到許多對研究有幫助的訊息。整個議程持續到當日下午 6 點結束。

美國時間 8 月 24 日星期三，早上 6 點便與飯店退房前往美國加州聖地牙哥國際機場搭乘回途班機。

二、 與會心得

此次參加於美國加州聖地牙哥舉行之國際光學工程學會-光電元件與應用 2011 (SPIE Photonic Devices + Applications 2011)研討會，在

第一天會程海報展示與說明時，遇到許多相同領域的博士班來自美國加州大學洛杉磯分校 UCLA 之 Yang Yang 教授學生、韓國 Heeger Center 的博士生以及許多學校之現役博士生，在互相展示彼此的研究成果與實驗上細節的討論，學習到許多不一樣的看法及知識也看到更多在此領域的最新研究成果，真的獲益良多。在議程演講的部分也有幸聆聽國際上此領域大師們的演講以及他們實驗室的研究成果與發展，讓本人對實驗上的進一步發展與規劃有了新的認知與見解，也對未來的下一步看到許多新的可能性。與會後的心得主要在高分子太陽能電池的下一步發展應該往高壽命以及耐大氣環境的新穎材料發展，但是也必須輔以元件製程上的進步和元件內部形態分布的解析，才可以完整發揮新材料的本質特性，以達到完整使用材料的最大效益與推展高分子太陽能電池的發展。

三、 建議

四、 攜回資料名稱與內容

1. SPIE Photonic Devices + Applications 2011 Technical Program
2. SPIE Photonic Devices + Applications 2011 Exhibition Guide

五、 其他

國立交通大學博士班研究生

出席國際會議報告

報告人姓名	江建銘	報告日期	100 年 08 月 31 日
系所及年級	材料所 博士班四年級	核定文號	100 年 06 月 30 日 11D121
連絡電話	03-5731771	電子信箱	Kensky706.mse97g@nctu.edu.tw
會議期間	100 年 08 月 21 日 到 100 年 08 月 25 日	會議地點	美國加州聖地牙哥
會議名稱	(中文) 國際光學工程學會-光電元件與應用 2011 (英文) SPIE Photonic Devices + Applications 2011		
發表論文題目	(中文) 合成具苯並呋喃之高開路電壓共軛高分子並應用於有機高分子太陽能電池。 (英文) High Open-Circuit Voltage Benzoxadiazole-Containing Polymers, Synthesis, Characterization and Photovoltaic Application.		

報告內容包括下列各項：

一、 參加會議經過

此次參加於美國加州聖地牙哥舉行之國際光學工程學會-光電元件

與應用 2011 (SPIE Photonic Devices + Applications 2011)，於 100 年 8 月 21 日出發並於美國時間 8 月 21 日星期日下午抵達飯店並且立即入住以後即先行前往會場確認會議議程。

美國時間 8 月 22 日星期一早上於十點抵達會場，並進行參加會議報到以及領取會議參加證件及相關文件，也一併把海報貼上所屬之欄位。當日下午便參予會議第一天之行程以及晚上海報展示與解說之活動，海報展示與解說之活動由下午 5 點半開始到 7 點半結束，於此活動以後便回到飯店結束此日之會議。

美國時間 8 月 23 日星期二，早上參加此趟會議之演講議程，此次分別有四個時段，其中演講者有美國史丹佛大學 Michael D.

McGehee、美國國家再生能源實驗室(NREL)、韓國 Kwanghee Lee 教授、台灣大學林清富教授等，許多此領域知名學者與會，並且得到許多對研究有幫助的訊息。整個議程持續到當日下午 6 點結束。

美國時間 8 月 24 日星期三，早上 6 點便與飯店退房前往美國加州聖地牙哥國際機場搭乘回途班機。

二、 與會心得

本次參與(SPIE Photonic Devices + Applications 2011)研討會在第一天海報展示及說明的過程中，與許多相同領域甚或不同領域

之研究人員在實驗上的細節及數據上之分析互相交流，學習到許多不同的觀點及實驗手法，同時亦得知許多在光電領域上最新的知識及發展，對未來實驗方向及設計方面相信有良好之之助益。在議程演講的部分也有幸聆聽國際上此領域大師們的演講及他們實驗室的研究成果與發展，讓本人對實驗上的進一步發展與規劃有了新的認知與見解，也對未來的下一步看到許多新的可能性。與會後的心得主要在高分子太陽能電池的下一步發展，除了目前發展之低能隙高分子以期達到全波段吸光、增加光電流外，應該往較低之氧化能階方向設計，以降低高分子之 HOMO 能階，使其提高開路電壓並增加高分子之抗氧化穩定性，提高壽命以及耐大氣環境的新穎材料發展，另外在高分子太陽能電池元件製作上，須輔以元件製程上的進步和元件內部形態分布的解析，才可以完整發揮新材料的本質特性，並往多層之元件結構設計，及反式元件製作法以達到完整使用材料的最大效益，並增加元件之存活時間與推展高分子太陽能電池的發展。

三、 建議

四、 攜回資料名稱與內容

1. SPIE Photonic Devices + Applications 2011 Technical Program

2. SPIE Photonic Devices + Applications 2011 Exhibition Guide

五、 其他

國科會補助計畫衍生研發成果推廣資料表

日期:2012/01/31

國科會補助計畫	計畫名稱: 奈米結構異質接面高分子太陽能電池之材料開發及元件設計(3/3)
	計畫主持人: 韋光華
	計畫編號: 99-2120-M-009-003- 學門領域: 奈米能源與環境技術
無研發成果推廣資料	

99 年度專題研究計畫研究成果彙整表

計畫主持人：韋光華		計畫編號：99-2120-M-009-003-					
計畫名稱：奈米結構異質接面高分子太陽能電池之材料開發及元件設計(3/3)							
成果項目		量化			單位	備註（質化說明：如數個計畫共同成果、成果列為該期刊之封面故事...等）	
		實際已達成數（被接受或已發表）	預期總達成數(含實際已達成數)	本計畫實際貢獻百分比			
國內	論文著作	期刊論文	0	0	100%	篇	
		研究報告/技術報告	0	0	100%		
		研討會論文	0	0	100%		
		專書	0	0	100%		
	專利	申請中件數	0	0	100%	件	
		已獲得件數	0	0	100%		
	技術移轉	件數	0	0	100%	件	
		權利金	0	0	100%	千元	
	參與計畫人力 (本國籍)	碩士生	5	5	100%	人次	
		博士生	6	6	100%		
		博士後研究員	0	0	100%		
		專任助理	0	0	100%		
國外	論文著作	期刊論文	20	15	100%	篇	
		研究報告/技術報告	0	0	100%		
		研討會論文	2	2	100%		
		專書	0	0	100%	章/本	
	專利	申請中件數	0	1	100%	件	
		已獲得件數	0	0	100%		
	技術移轉	件數	0	0	100%	件	
		權利金	0	0	100%	千元	
	參與計畫人力 (外國籍)	碩士生	0	0	100%	人次	
		博士生	0	0	100%		
		博士後研究員	0	0	100%		
		專任助理	0	0	100%		

<p>其他成果 (無法以量化表達之成果如辦理學術活動、獲得獎項、重要國際合作、研究成果國際影響力及其他協助產業技術發展之具體效益事項等，請以文字敘述填列。)</p>	無。
--	----

	成果項目	量化	名稱或內容性質簡述
科 教 處 計 畫 加 填 項 目	測驗工具(含質性與量性)	0	
	課程/模組	0	
	電腦及網路系統或工具	0	
	教材	0	
	舉辦之活動/競賽	0	
	研討會/工作坊	0	
	電子報、網站	0	
	計畫成果推廣之參與(閱聽)人數	0	

國科會補助專題研究計畫成果報告自評表

請就研究內容與原計畫相符程度、達成預期目標情況、研究成果之學術或應用價值（簡要敘述成果所代表之意義、價值、影響或進一步發展之可能性）、是否適合在學術期刊發表或申請專利、主要發現或其他有關價值等，作一綜合評估。

1. 請就研究內容與原計畫相符程度、達成預期目標情況作一綜合評估

達成目標

未達成目標（請說明，以 100 字為限）

實驗失敗

因故實驗中斷

其他原因

說明：

2. 研究成果在學術期刊發表或申請專利等情形：

論文： 已發表 未發表之文稿 撰寫中 無

專利： 已獲得 申請中 無

技轉： 已技轉 洽談中 無

其他：（以 100 字為限）

3. 請依學術成就、技術創新、社會影響等方面，評估研究成果之學術或應用價值（簡要敘述成果所代表之意義、價值、影響或進一步發展之可能性）（以 500 字為限）

無